



CT Image Segmentation Using Optimization Techniques under Neutrosophic Domain

Doaa El-Shahat ^{1,*} , Nourhan Talal ¹ , Jun Ye ^{2,3} , and Wen-Hua Cui ³ 

¹ Department of Computer Science, Faculty of Computers and Informatics, Zagazig University, Zagazig 44519, Egypt;

Emails: doaazidan@zu.edu.eg; N.Talal22@fci.zu.edu.eg.

² School of Civil and Environmental Engineering, Ningbo University, Ningbo, Zhejiang, China; yejun1@nbu.edu.cn.

³ Department of Electrical Engineering and Automation, Shaoxing University, Shaoxing, Zhejiang, China; wenhuacui@usx.edu.cn.

* Correspondence: doaazidan@zu.edu.eg

Abstract: In this paper, we introduce a hybrid technique between optimization algorithms and neutrosophic theory. This new hybridization can deal with uncertainties in brain computed tomography (CT) images in three different memberships very effectively. To prove the real-time application of this theory, a new segmentation method for brain CT medical images is presented. The grayscale medical image suffers from uncertainties and inconsistencies in the gray levels due to their bad luminance. The proposed technique addressed this problem by performing neutrosophic operations on gray levels based on the S membership function.

Keywords: Neutrosophic Set; CT Image Segmentation; Medical Images; Optimization Algorithms.

1. Introduction

The segmentation process in medicine aims to extract the region of interest (ROI) object (organ) from a medical image (2D or 3D). It separates an image into regions according to a given outline, for example, segmenting human tissues or organs in medical applications for border detection, tumor detection/segmentation, and mass detection [1]. Furthermore, computed tomography (CT) medical imaging suffers from different uncertainty problems that affect the process of image segmentation. A CT is a gray-level image with large amounts of noise and a low level of intensity. Additionally, CT has poor edge representation and contrast regions. With so little data and low-quality images. These problems pose a challenge in the segmentation process because they can degrade the efficiency of the whole image processing operation. So, it's important to use methods that can handle and deal with uncertain information within images [2]

The fuzzy set (FS), intuitionistic fuzzy set (IFS), and neutrosophic set (NS) were developed to deal with uncertainties. FS theory was introduced by Zadeh to deal with uncertainty based on the degree of membership [3]. The FS theory is used widely in medical image segmentation. Zhang et al. [4] proposed the Reference-guided Fuzzy Integral GAN (RFI-GAN) generating ultrasound images by combining feature fusion between samples and reference sets. It generalizes feature additivity to non-additivity using fuzzy integral. Two Fuzzy Integral Modules are proposed for the nonlinear fusion of texture and structure features. Another contribution by Zhao et al. [5] presents a BLS surrogate-assisted evolutionary framework for improving time efficiency in clustering-based image segmentation. The BLS-MOEF algorithm uses two fuzzy clustering objective functions, a BLS surrogate model-assisted multi-objective evolutionary framework, adaptive parameter updating, and a novel fuzzy clustering validity index. Also, Kumar et al. [6] introduced a new CoMHisP framework using a fuzzy support vector machine (SVM) with within-class density information. It extracts image micropatterns and computes the center of mass for each pixel. The framework performs well on a CMT dataset of histopathological images of canine mammary tumors and human

breast cancer. It achieves a classification accuracy of 97.25%, outperforming traditional ML and deep FE-VGGNET16-based feature descriptors.

In 1986, Atanassov introduced the IFS, which links each attribute in the universe with membership (M) and non-membership (non-M) degrees [7]. Kumar et al. [8] proposed an optimization problem for the IFCM with spatial neighborhood information (IFCMSNI) method, incorporating intuitionistic fuzzy set theory and spatial regularization to handle noise in medical images. The method uses IFS and Sugeno's negation function. Also, Namburu et al. [9] proposed a simplified clustering method for melanoma detection, using the triangular membership function (TMF) to identify initial regions and intuitionistic fuzzy c-means clustering, achieving an average accuracy of 90%. Dahiya and Anjana Gosain [10] introduced a novel Type-II intuitionistic fuzzy C means clustering algorithm, combining Type-II membership with a hesitation degree. This algorithm offers advantages such as clear cluster definition, robustness to noise and outliers, and improved centroids' desired position. Compared to other fuzzy clustering algorithms, it outperforms others in accurately identifying lump shape and size in mammograms. The algorithm reduces the average error by 84% on synthetic data sets.

The segmentation methods goal under the FS, and IFS environment is to deal with the uncertainties within an image, but they suffer from some problems such as:

- The segmentation approaches under the FS environment handle uncertainty by taking into consideration only the membership degree for image pixel values between $[0,1]$.
- The segmentation approaches under the FS environment handle uncertainty by taking into consideration only a hesitant degree in conditions of 'Membership' and "Non-Membership" degrees of image pixel values.

Smarandache [11] proposed NS to associate each element with a {truth membership, Indeterminacy membership, and falsity membership} function independently. The NS has values ranging $]^{-0,1^{+}}$ on real standard or non-standard subsets. Many applications can deal with the interval $[0,1]$ because dealing with $]^{-0,1^{+}}$ in real situations is difficult [12].

On the other hand, a variety of segmentation approaches have been developed to address CT image segmentation, ranging from conventional methods to swarm intelligence techniques and metaheuristics. Anter et al. [13] proposed a dynamic approach to improve the fuzzy c-means clustering algorithm for automatic localization and segmentation of liver and hepatic lesions from CT scans. The approach uses fast-FCM, chaos theory, and bio-inspired ant lion optimizer (ALO) to determine optimal cluster centroids. Another contribution presented a novel multi-disease diagnosis model using chest X-ray images using deep learning approaches. The model uses standard datasets, pre-processing, segmentation, and classification using Optimized DeepLabv3, optimized by the Mutation Rate-based Lion Algorithm (MR-LA). The model improves sensitivity, precision, and specificity, achieving higher classification and detection accuracy. The recommended method outperforms other models in relative analysis [14]. Chouksey et al. [15] investigated the effectiveness of antlion optimization (ALO) and multiverse optimization (MVO), two nature-inspired algorithms, in detecting tumors in medical images. ALO mimics antlion hunting behavior, while MVO is based on multiverse theory. The proposed algorithm outperforms other evolutionary algorithms and is faster than MVO. The results are analyzed using a Wilcoxon test.

The previous studies have outlined some challenges in CT brain segmentation:

- The segmentation technique is complicated by bias areas and inconsistent borders present in CT images.
- Unfortunately, several factors make the segmentation of CT images difficult, including the patient's condition, and operator error.
- The increasing dimension of membership functions may pose challenges for high precision in addressing uncertainty.

These problems highlight the critical need for a more thorough method in medical image segmentation to effectively handle fuzziness and uncertainty in CT brain images. This study presented a segmentation strategy based on optimization techniques under the NS domain. A comparison between Differential Evolution (DE), Spider Wasp Optimization (SWO), Grey Wolf Optimizer (GWO), Particle Swarm Optimization (PSO), and Whale Optimization Algorithm (WOA) optimization algorithm under the NS domain was implemented.

Consequently, the following are this paper's main contributions:

- Propose a segmentation approach based on NS that can deal with uncertainty by presenting a degree of indeterminacy.
- Compare five optimization algorithms under the NS domain.
- The NS image is obtained from the image guided by a DE, SWO, GWO, PSO, and WOA for optimized clustering for segmenting the medical images with reduced time consumption and efficient accuracy.

The remainder of the paper is divided as follows. Section 2 provides the background needed for this study. Section 3 presents preliminaries for neutrosophic theory and optimization algorithms. Section 4 presents the steps of the proposed approach. Section 5 presents experimental results. Section 6 illustrates the conclusion and future directions of this proposal.

2. Related Work

Many studies aim to integrate NS with optimization and metaheuristics methods. Palanisamy et al. [16] proposed a method using NS combined with fuzzy c-means clustering (FCM) and modified particle swarm optimization (PSO) for brain tumor segmentation, achieving superior sensitivity, specificity, Jaccard, and dice values compared to FCM alone and FCM with NS. Ashour et al. [17] introduced a skin lesion detection method called optimized neutrosophic k-means (ONKM), based on genetic algorithms. The method optimizes the neutrosophic set operation to reduce indeterminacy in dermoscopy images. The Jaccard index is used as the fitness function. The ONKM method is applied to segment dermoscopy images, and its performance is evaluated using metrics like Dice coefficient, specificity, sensitivity, and accuracy. The ONKM method outperforms k-means and y-k-means methods in accuracy.

Another contribution by Anter et al. [18] proposed a segmentation approach for abdominal CT liver tumors using neutrosophic sets, PSO, and fast fuzzy C-mean algorithm (FFCM). The method involves removing intensity values and high frequencies, transforming the image to the NS domain, optimizing FFCM using PSO, and clustering the livers using PSOFCCM. The results showed neutrosophic sets offer accurate, less time-consuming, and noise-sensitive segmentation on non-uniform CT images.

Sayed et al. [19] presented an automatic mitosis detection approach for histopathology slide imaging using NS and moth-flame optimization (MFO). The approach involves two phases: candidate extraction and classification. The Gaussian filter is applied to the image, and morphological operations are applied to enhance it. The best features are selected using the meta-heuristic MFO algorithm. The approach is tested on a benchmark dataset of 50 histopathological images, including breast pathology slides. The results show the MFO feature selection algorithm maximizes classification performance, with high accuracy, recall, precision, and f-score.

Hanbay and Talu [20] introduces a novel SAR image segmentation algorithm based on the neutrosophic set and an improved artificial bee colony (I-ABC) algorithm. The algorithm uses threshold value estimation to search for a proper value in grayscale intervals. The I-ABC optimization algorithm is used to find the optimal threshold value. The paper contributes to SAR image segmentation by introducing a hybrid model with two feature extraction methods and demonstrating its effectiveness in real SAR images.

Another study introduced a new methodology for license plate (LP) recognition using image processing algorithms and an optimized neutrosophic set (NS) based on genetic algorithm (GA). The methodology uses edge detection, morphological operations, and a new methodology using GA to optimize NS operations. The k-means clustering algorithm and connected components labeling analysis (CCLA) algorithm are used to segment characters. The proposed methodology is suitable for both Arabic-Egyptian and English LP, achieving high recognition accuracy in high-resolution Egyptian and low-resolution-corrupted English. The system also achieves 92.5% accuracy in image disturbances [21].

From previous studies, we conclude that

- No studies are comparing different optimization techniques under the neutrosophic domain.
- Few studies investigate the results of hybrid NS and optimization in medical images.

3. Neutrosophic Sets

The NS can deal with uncertainty and fuzziness within any data by describing the attribute with three components such as the True (T), Indeterminate(I), False (F) subsets. The CT images are mapped into the NS domain. Where a pixel P in the image is defined as $P(T, I, F)$ where t , i , and f are the true, indeterminate, and false in the set, respectively, as t diverges in T, i diverges in I, and f diverges in F. Then, the pixel $P(x, y)$ in the image space is transformed into the NS space $P_{NS}(x, y) = \{T(x, y), I(x, y), F(x, y)\}$. $T(x, y)$, $I(x, y)$ and $F(x, y)$ are the corresponding probabilities which are given by [27]:

$$T(x, y) = \frac{\bar{g}(x, y) - \bar{g}_{min}}{\bar{g}_{max} - \bar{g}_{min}} \quad (1)$$

$$\bar{g}(x, y) = \left(\frac{1}{w \times w} \right) \sum_{m=a-\frac{w}{2}}^{a+\frac{w}{2}} \sum_{n=i-\frac{w}{2}}^{i+\frac{w}{2}} g(m, n) \quad (2)$$

$$F(x, y) = 1 - T(x, y) \quad (3)$$

$$\delta(x, y) = \text{abs}(g(x, y) - \bar{g}(x, y)) \quad (4)$$

$$I(x, y) = \frac{\delta(x, y) - \delta_{min}}{\delta_{max} - \delta_{min}} \quad (5)$$

where the pixels in the window have $\bar{g}(x, y)$ local mean, and $\delta(x, y)$ implies the absolute value of difference among intensity $g(x, y)$ and its $\bar{g}(x, y)$.

The entropy is computed for a grayscale image to evaluate the distribution of gray levels. When the intensities have a uniform distribution and equal probability, maximum entropy occurs. When intensities have nonuniform distribution and varying probabilities, little entropy arises. The totality of the T, I, and F entropies is referred to as the entropy in the neutrosophic image, and it is used to calculate the element distribution in the NS domain [27]. The entropy can be donated by the following

$$Entropy_{NS} = Entropy_T + Entropy_I + Entropy_F \quad (6)$$

$$Entropy_T = - \sum_{j=\min\{T\}}^{\max\{T\}} P_T(K) \ln P_T(k) \quad (7)$$

$$Entropy_I = - \sum_{j=\min\{I\}}^{\max\{I\}} P_I(K) \ln P_I(k) \quad (8)$$

$$Entropy_F = - \sum_{j=\min\{F\}}^{\max\{F\}} P_F(K) \ln P_F(k) \quad (9)$$

where the entropies are $Entropy_T$, $Entropy_I$, and $Entropy_F$ for T, I, and F, respectively. Furthermore, the probabilities of the element k are $P_T(K)$, $P_I(K)$, and $P_F(K)$ in T, I, and F, respectively.

4. Proposed Algorithm

The neutrosophic set theory allows us to handle uncertainties, imprecision, and vagueness in image data. By combining optimization algorithms with neutrosophic image segmentation, we can improve the adaptability of the segmentation process to different image types and conditions. Optimization algorithms can also help refine the segmentation process by iteratively adjusting the parameters of some membership functions to maximize the entropy, thereby aiding in segmenting the images more accurately. In this study, we employ the S membership function to generate both T and F domains in NS theory. This function is mathematically defined as follows:

$$T(\bar{g}(x, y), a, b, c) = \begin{cases} 0, & \bar{g}(x, y) \leq a \\ \frac{(\bar{g}(x, y) - a)^2}{(b - a)(c - a)}, & a \leq \bar{g}(x, y) \leq b \\ 1 - \frac{(\bar{g}(x, y) - c)^2}{(c - b)(c - a)}, & b \leq \bar{g}(x, y) \leq c \\ 1, & \bar{g}(x, y) \geq c \end{cases} \quad (10)$$

where a , b , and c are three parameters that need to be accurately estimated to better separate the true and false NS domains. $Entropy_T$ is used as an objective function to be optimized for reaching the near-optimal values for those parameters. To perform this optimization process, the DE algorithm is herein employed due to its high performance and stability for several optimization problems [22].

5. Results and Discussion

This section assesses the performance of the DE algorithm when applied to search for the near-optimal intervals of the S membership function that could accurately segment the true (object) and false (background) NS domains from eight brain tumor MRI images. The MRI images used in our experiments are shown in Table 1. The performance of this algorithm is compared to four metaheuristic algorithms, such as spider wasp optimizer (SWO) [23], grey wolf optimizer (GWO) [24], particle swarm optimization (PSO) [25], and whale optimization algorithm (WOA) [26] in terms of four performance metrics, such as best entropy, worst entropy, average (Avg) entropy, and standard deviation (SD). All algorithms are executed 25 independent times, and those performance metrics are computed under the estimated outcomes and reported in Table 2. Inspecting this table shows that DE is the highest-performing algorithm because it could achieve the best outcomes for all test images. To show those findings more clearly, Figure 1 is presented to compute the average entropy obtained by each algorithm on all test images. From this figure, DE is the best, WOA is the second best, and PSO is the worst algorithm. Table 3 displays the NS domains for three test images obtained by the intervals optimized by DE. Finally, Figure 2 shows the convergence curves of various algorithms on three test images, showing the superiority of DE.

Table 1. Brain tumor MRI images used in this study.

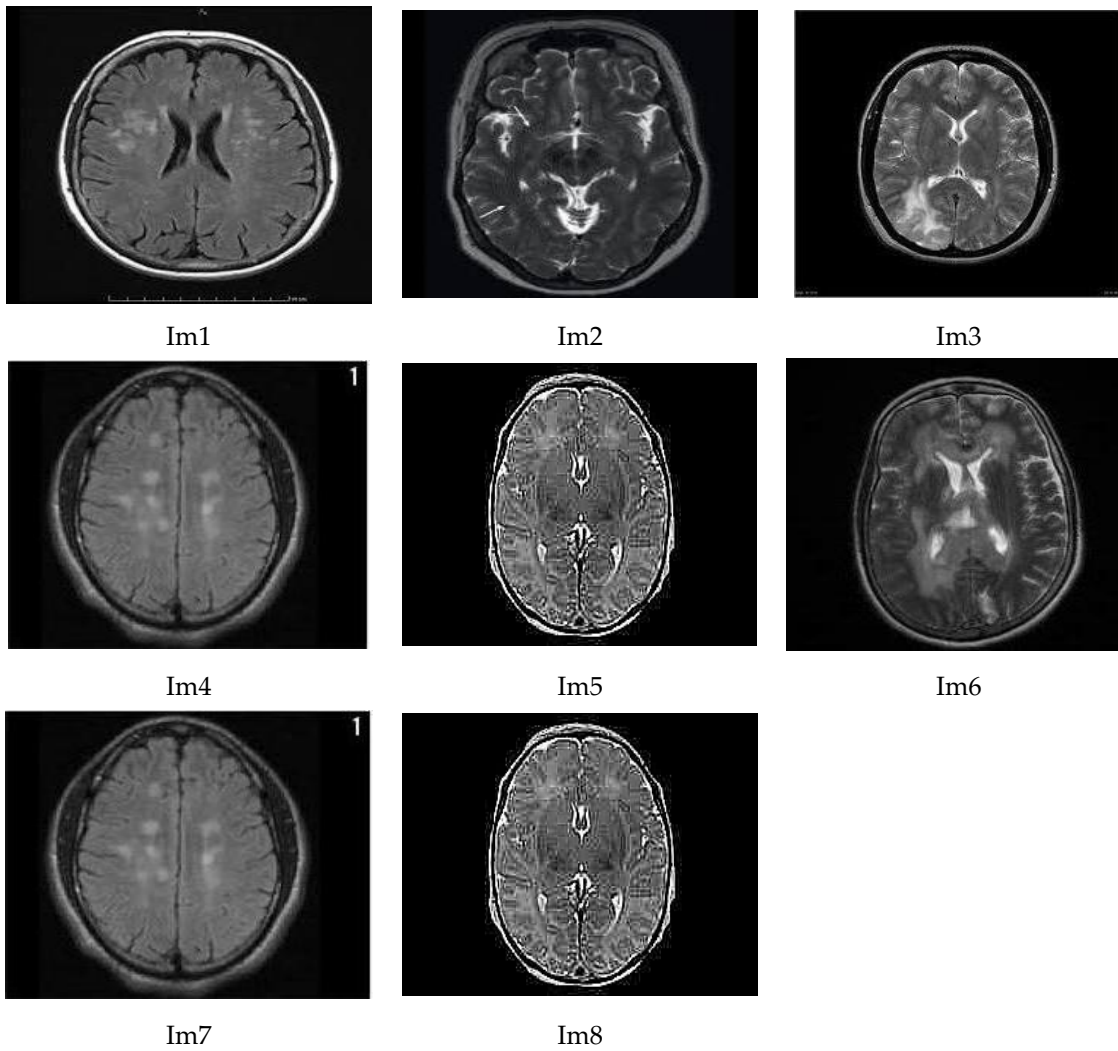


Table 2. Comparison among algorithms under various performance indicators.

		DE	GWO	SWO	PSO	WOA
Im1	Worst	0.620686	0.415060	0.444266	0.398349	0.471238
	Avg	0.677270	0.574949	0.490833	0.488476	0.627003
	Best	0.680248	0.680248	0.539082	0.647501	0.680248
	SD	0.013318	0.071869	0.026369	0.050946	0.077810
Im2	Worst	0.642074	0.493266	0.442960	0.030411	0.457366
	Avg	0.654727	0.596860	0.501641	0.462250	0.624038
	Best	0.661597	0.661484	0.563887	0.659975	0.661602
	SD	0.007790	0.050992	0.033069	0.188853	0.055873
Im3	Worst	0.402475	0.276877	0.292270	0.295417	0.318098
	Avg	0.402475	0.354111	0.342486	0.324730	0.368765
	Best	0.402475	0.393584	0.387712	0.384954	0.402475
	SD	0.000000	0.033357	0.026493	0.021967	0.031272
Im4	Worst	0.550052	0.395324	0.432564	0.356642	0.458786
	Avg	0.593570	0.508910	0.481033	0.468366	0.560984
	Best	0.598151	0.582767	0.565751	0.568650	0.598151
	SD	0.014121	0.048259	0.036770	0.042583	0.048622
Im5	Worst	0.369277	0.300446	0.351128	0.340329	0.350936
	Avg	0.389828	0.371943	0.372858	0.366689	0.374335
	Best	0.391531	0.391531	0.386141	0.387104	0.391531
	SD	0.005029	0.019334	0.010194	0.012415	0.013341
Im6	Worst	0.533367	0.394530	0.338283	0.037360	0.380744
	Avg	0.535418	0.480866	0.432992	0.399207	0.488436
	Best	0.536576	0.529927	0.490044	0.528113	0.536576
	SD	0.001156	0.042239	0.032867	0.105190	0.060838
Im7	Worst	0.320014	0.256615	0.244669	0.205086	0.264061
	Avg	0.336299	0.292112	0.274215	0.262058	0.300279
	Best	0.337156	0.337156	0.308615	0.305846	0.337156
	SD	0.003833	0.024531	0.017462	0.025219	0.023771
Im8	Worst	0.589639	0.428177	0.360343	0.334022	0.481198
	Avg	0.630500	0.526989	0.424768	0.403364	0.601137
	Best	0.635223	0.635223	0.503232	0.478930	0.635223
	SD	0.012705	0.052780	0.040396	0.033492	0.057329

Bold values indicate the best findings.

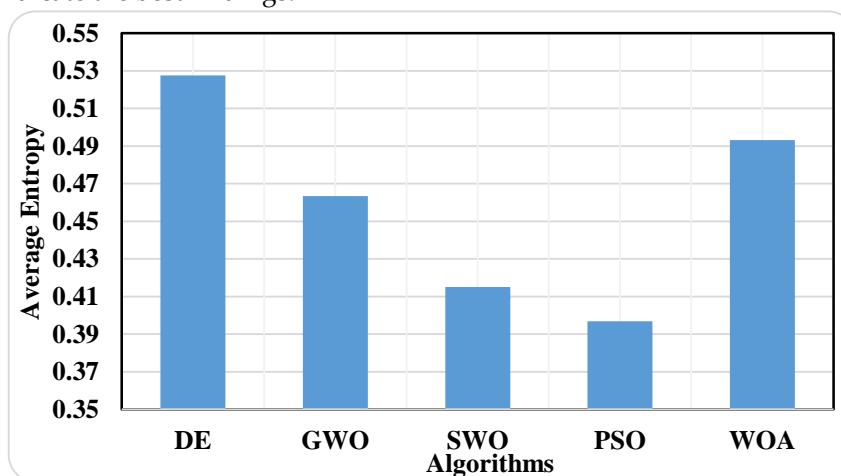
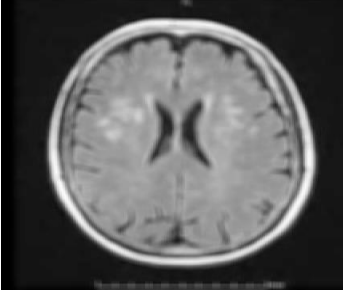
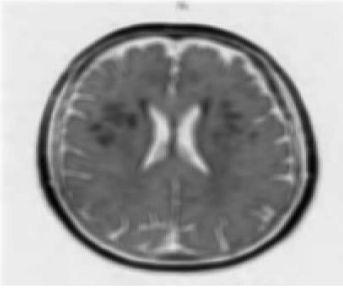
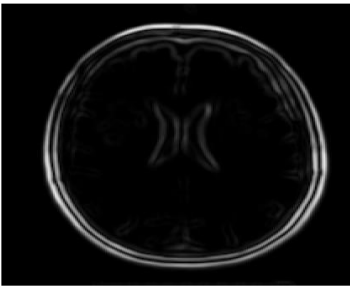
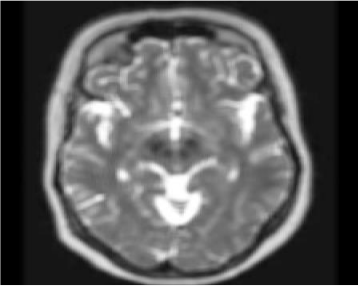
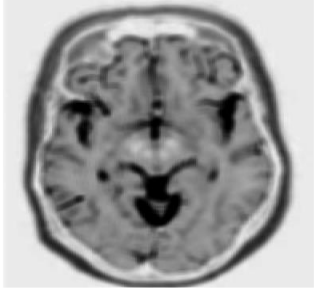
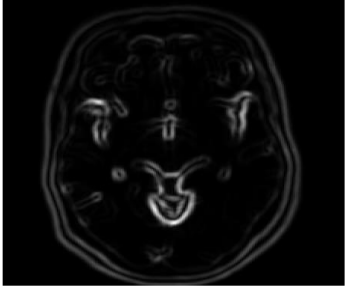
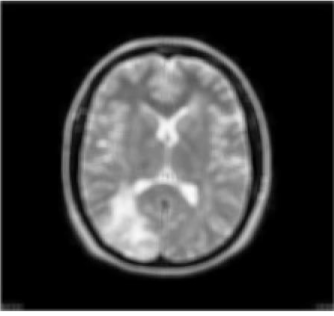

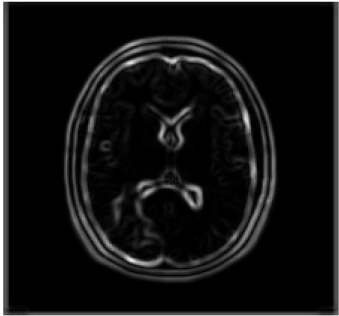
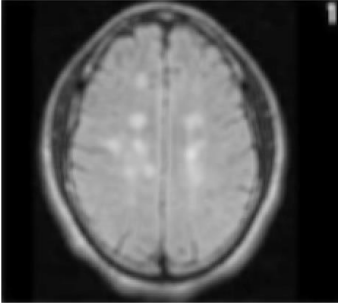
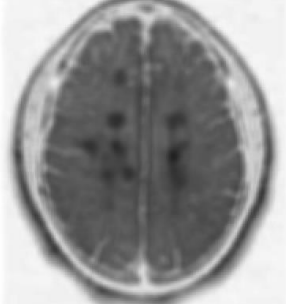
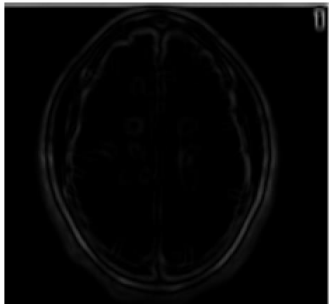


Figure 1. Average entropy obtained by each algorithm on all test images.

Table 3. Depiction of NS domains for four test images obtained after applying the DE algorithm.

		
T-domain for im1	F-domain for im1	I-domain for im1
		
T-domain for im2	F-domain for im2	I-domain for im2
		
T-domain for im3	F-domain for im3	I-domain for im3
		
T-domain for im4	F-domain for im4	I-domain for im4

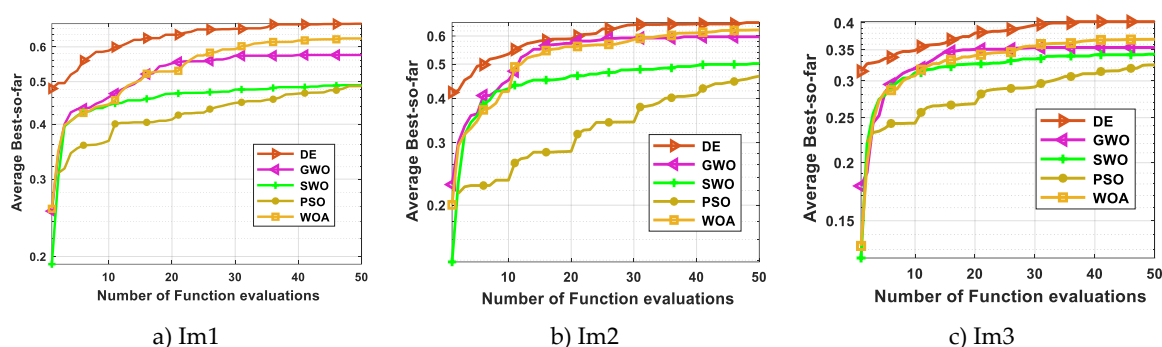


Figure 2. Convergence curves obtained by various algorithms on three test images.

6. Conclusion and Future Work

In this paper, a novel segmentation algorithm based on a Neutrosophic set and optimization techniques has been introduced. The applicability of the image segmentation under the neutrosophic domain was demonstrated on CT images. In our approach, Neutrosophic was obtained to transform the grayscale CT image to the NS domain and measure uncertainties using Neutrosophic entropy. The experiments were presented on 8 CT images.

Acknowledgments

The author is grateful to the editorial and reviewers, as well as the correspondent author, who offered assistance in the form of advice, assessment, and checking during the study period.

Author Contributions

All authors contributed equally to this research.

Data availability

The datasets generated during and/or analyzed during the current study are not publicly available due to the privacy-preserving nature of the data but are available from the corresponding author upon reasonable request.

Funding

This research was not supported by any funding agency or institute.

Conflict of interest

The authors declare that there is no conflict of interest in the research.

References

1. Yan, L., Zhao, H., Lin, Y., & Sun, Y. (2023). Basic Theory of Remote Sensing Digital Image Pixel Processing II: Time–Frequency Fourier Transform from Convolution to Multiplication. In *Math Physics Foundation of Advanced Remote Sensing Digital Image Processing* (pp. 157-187). Singapore: Springer Nature Singapore. https://doi.org/10.1007/978-981-99-1778-5_6
2. Baumgartner, C. F., Tezcan, K. C., Chaitanya, K., Hötker, A. M., Muehlematter, U. J., Schawkat, K., & Konukoglu, E. (2019). Phiseg: Capturing uncertainty in medical image segmentation. In *Medical Image Computing and Computer Assisted Intervention–MICCAI 2019: 22nd International Conference, Shenzhen, China, October 13–17, 2019, Proceedings, Part II 22* (pp. 119-127). Springer International Publishing. https://doi.org/10.1007/978-3-030-32245-8_14
3. Zadeh, L. A. (1978). Fuzzy sets as a basis for a theory of possibility. *Fuzzy sets and systems*, 1(1), 3-28. [https://doi.org/10.1016/0165-0114\(78\)90029-5](https://doi.org/10.1016/0165-0114(78)90029-5)
4. Zhang, R., Lu, W., Gao, J., Tian, Y., Wei, X., Wang, C., & Yu, M. (2023). RFI-GAN: A reference-guided fuzzy integral network for ultrasound image augmentation. *Information Sciences*, 623, 709-728. <https://doi.org/10.1016/j.ins.2022.12.026>

5. Zhao, F., Liu, Y., Liu, H., & Fan, J. (2022). Broad learning approach to Surrogate-Assisted Multi-Objective evolutionary fuzzy clustering algorithm based on reference points for color image segmentation. *Expert Systems with Applications*, 200, 117015. <https://doi.org/10.1016/j.eswa.2022.117015>
6. Kumar, A., Singh, S. K., Saxena, S., Singh, A. K., Shrivastava, S., Lakshmanan, K., & Singh, R. K. (2020). CoMHisP: A novel feature extractor for histopathological image classification based on fuzzy SVM with within-class relative density. *IEEE Transactions on Fuzzy Systems*, 29(1), 103-117. <https://doi.org/10.1109/TFUZZ.2020.2995968>
7. Atanassov, K. T. (1999). *Intuitionistic fuzzy sets* (pp. 1-137). Springer, Physica-Verlag HD.
8. Kumar, D., Agrawal, R. K., & Kirar, J. S. (2019, June). Intuitionistic fuzzy clustering method with spatial information for mri image segmentation. In 2019 IEEE international conference on fuzzy systems (FUZZ-IEEE) (pp. 1-7). IEEE. <https://doi.org/10.1109/FUZZ-IEEE.2019.8858865>
9. Namburu, A., Mohan, S., Chakkaravarthy, S., & Selvaraj, P. (2023). Skin Cancer Segmentation Based on Triangular Intuitionistic Fuzzy Sets. *SN Computer Science*, 4(3), 228. <https://doi.org/10.1007/s42979-023-01701-8>
10. Dahiya, S., & Gosain, A. (2023). A novel type-II intuitionistic fuzzy clustering algorithm for mammograms segmentation. *Journal of Ambient Intelligence and Humanized Computing*, 14(4), 3793-3808. <https://doi.org/10.1007/s12652-022-04022-5>
11. Smarandache, F. (2002, January). Preface: an introduction to neutrosophy, neutrosophic logic, neutrosophic net, and neutrosophic probability and statistics. In *Proceedings of the first international conference on Neutrosophy, neutrosophic logic, neutrosophic set, neutrosophic probability and statistics* (pp. 5-21).
12. Mohan, J., Krishnaveni, V., & Guo, Y. (2013). A new neutrosophic approach of Wiener filtering for MRI denoising. *Measurement Science Review*, 13(4), 177-186.
13. Anter, A. M., Bhattacharyya, S., & Zhang, Z. (2020). Multi-stage fuzzy swarm intelligence for automatic hepatic lesion segmentation from CT scans. *Applied Soft Computing*, 96, 106677. <https://doi.org/10.1016/j.asoc.2020.106677>
14. Balmuri, K. R., Konda, S., kumar Mamidala, K., & Gunda, M. (2024). Automated and reliable detection of multi-diseases on chest X-ray images using optimized ensemble transfer learning. *Expert Systems with Applications*, 246, 122810. <https://doi.org/10.1016/j.eswa.2023.122810>
15. Chouksey, M., Jha, R. K., & Sharma, R. (2020). A fast technique for image segmentation based on two meta-heuristic algorithms. *Multimedia tools and applications*, 79(27), 19075-19127. <https://doi.org/10.1007/s11042-019-08138-3>
16. Palanisamy, T. S. C. A., Jayaraman, M., Vellingiri, K., & Guo, Y. (2019). Optimization-based neutrosophic set for medical image processing. In *Neutrosophic set in medical image analysis* (pp. 189-206). Academic Press. <https://doi.org/10.1016/B978-0-12-818148-5.00009-6>
17. Ashour, A. S., Hawas, A. R., Guo, Y., & Wahba, M. A. (2018). A novel optimized neutrosophic k-means using genetic algorithm for skin lesion detection in dermoscopy images. *Signal, Image and Video Processing*, 12(7), 1311-1318. <https://doi.org/10.1007/s11760-018-1284-y>
18. Anter, A. M., & Hassenian, A. E. (2018). Computational intelligence optimization approach based on particle swarm optimizer and neutrosophic set for abdominal CT liver tumor segmentation. *Journal of Computational Science*, 25, 376-387. <https://doi.org/10.1016/j.jocs.2018.01.003>
19. Sayed, G. I., & Hassanien, A. E. (2017). Moth-flame swarm optimization with neutrosophic sets for automatic mitosis detection in breast cancer histology images. *Applied Intelligence*, 47, 397-408. <https://doi.org/10.1007/s10489-017-0897-0>
20. Hanbay, K., & Talu, M. F. (2014). Segmentation of SAR images using improved artificial bee colony algorithm and neutrosophic set. *Applied Soft Computing*, 21, 433-443. <https://doi.org/10.1016/j.asoc.2014.04.008>
21. Yousif, B. B., Ata, M. M., Fawzy, N., & Obaya, M. (2020). Toward an optimized neutrosophic K-means with genetic algorithm for automatic vehicle license plate recognition (ONKM-AVLPR). *IEEE Access*, 8, 49285-49312. <https://doi.org/10.1109/ACCESS.2020.2979185>
22. Price, K. V., Storn, R. M., & Lampinen, J. A. (2005). The differential evolution algorithm. *Differential evolution: a practical approach to global optimization*, 37-134.

23. Abdel-Basset, M., Mohamed, R., Jameel, M., & Abouhawwash, M. (2023). Spider wasp optimizer: A novel meta-heuristic optimization algorithm. *Artificial Intelligence Review*, 56(10), 11675-11738. <https://doi.org/10.1007/s10462-023-10446-y>
24. Faris, H., Aljarah, I., Al-Betar, M. A., & Mirjalili, S. (2018). Grey wolf optimizer: a review of recent variants and applications. *Neural computing and applications*, 30, 413-435. <https://doi.org/10.1007/s00521-017-3272-5>
25. Aje, O. F., & Josephat, A. A. (2020). The particle swarm optimization (PSO) algorithm application–A review. *Global Journal of Engineering and Technology Advances*, 3(3), 001-006. <https://doi.org/10.30574/gjeta.2020.3.3.0033>
26. Mirjalili, S., & Lewis, A. (2016). The whale optimization algorithm. *Advances in engineering software*, 95, 51-67. <https://doi.org/10.1016/j.advengsoft.2016.01.008>
27. Guo, Y., Cheng, H. D., & Zhang, Y. (2009). A new neutrosophic approach to image denoising. *New Mathematics and Natural Computation*, 5(03), 653-662. <https://doi.org/10.1142/S1793005709001490>

Received: 02 Dec 2023, **Revised:** 01 Mar 2024,

Accepted: 27 Mar 2024, **Available online:** 01 Apr 2024.



© 2024 by the authors. Submitted for possible open access publication under the terms and conditions of the Creative Commons Attribution (CC BY) license (<http://creativecommons.org/licenses/by/4.0/>).

Disclaimer/Publisher's Note: The perspectives, opinions, and data shared in all publications are the sole responsibility of the individual authors and contributors, and do not necessarily reflect the views of Sciences Force or the editorial team. Sciences Force and the editorial team disclaim any liability for potential harm to individuals or property resulting from the ideas, methods, instructions, or products referenced in the content.